IL-17A Influences Essential Functions of the Monocyte/Macrophage Lineage and Is Involved in Advanced Murine and Human Atherosclerosis

Christian Erbel,* Mohammadreza Akhavanpoor,* Deniz Okuyucu,* Susanne Wangler,* Alex Dietz,* Li Zhao,* Konstantinos Stellos,† Kristina M. Little,‡ Felix Lasitschka,§ Andreas Doesch,* Maani Hakimi,¶,‖ Thomas J. Dengler,# Thomas Giese, Erwin Blessing,* Hugo A. Katus,*,†† and Christian A. Gleissner***

Atherosclerosis is a chronic inflammatory disease. Lesion progression is primarily mediated by cells of the monocyte/macrophage lineage. IL-17A is a proinflammatory cytokine, which modulates immune cell trafficking and is involved inflammation in (auto)immune and infectious diseases. But the role of IL-17A still remains controversial. In the current study, we investigated effects of IL-17A on advanced murine and human atherosclerosis, the common disease phenotype in clinical care. The 26-wk-old apolipoprotein E–deficient mice were fed a standard chow diet and treated either with IL-17A mAb (n = 15) or irrelevant Ig (n = 10) for 16 wk. Furthermore, essential mechanisms of IL-17A in atherogenesis were studied in vitro. Inhibition of IL-17A markedly prevented atherosclerotic lesion progression (p = 0.001) by reducing inflammatory burden and cellular infiltration (p = 0.01) and improved lesion stability (p = 0.01). In vitro experiments showed that IL-17A plays a role in chemoattractance, monocyte adhesion, and sensitization of APCs toward pathogen-derived TLR4 ligands. Also, IL-17A induced a unique transcriptome pattern in monocyte-derived macrophages distinct from known macrophage types. Stimulation of human carotid plaque tissue ex vivo with IL-17A induced a proinflammatory milieu and upregulation of molecules expressed by the IL-17A–induced macrophage subtype. In this study, we show that functional blockade of IL-17A prevents atherosclerotic lesion progression and induces plaque stabilization in advanced lesions in apolipoprotein E–deficient mice. The underlying mechanisms involve reduced inflammation and distinct effects of IL-17A on monocyte/macrophage lineage. In addition, translational experiments underline the relevance for the human system. ***The Journal of Immunology*****, 2014, 193: 4344–4355.**

Progressive atherosclerosis, the leading cause of death and disability worldwide, may lead to rupture of vulnerable vascular plaques, causing atherothrombosis and vessel occlusion (1). Chronic inflammatory processes are important mechanisms that lead to atherosclerotic lesion development and progression (1). Recent studies have shown that plaque progression is predominantly caused by monocyte recruitment and/or local proliferation of macrophages (2, 3), whereas plaque stabilization and regression is characterized by reduced macrophage accumulation due to predominantly reduced monocyte recruitment, but also migratory egress of macrophages (4).

The proinflammatory cytokine IL-17A modulates immune cell trafficking, mainly through induction of chemokines, thereby initiating inflammation and cytokine production in several autoimmune diseases (5, 6). IL-17A is produced by various inflammatory cells, including T cells and macrophages, and modulates the expression of several proinflammatory molecules (TNF-α, IL-1β, and CCL2 [MCP-1]) and matrix metalloproteinases (5, 7). Previously, our group and others (7–11) have shown that inhibition of IL-17A influenced atherosclerotic lesion development in mice with partially controversial results. Because the highest expression rates of IL-17A were observed in human carotid artery plaques derived from symptomatic patients with stroke or transient ischemic attack (12, 13), IL-17A may be linked to vulnerability of human atherosclerotic lesions.

The goal of the present work was to study the effects of IL-17A on advanced lesion progression, the common disease phenotype in clinical care, in apolipoprotein E–deficient ($Apoe^{-/-}$) mice, additional effects on atherogenic cells, and translation to the human system.

Materials and Methods

Animals

Male $Apoe^{-/-}$ mice 26 wk of age (strain B6.129P2) on a C57BL/6J background (n = 30) were kept within the animal care facility of the

*Department of Cardiology, University of Heidelberg, Heidelberg 69120, Germany; †Institute of Cardiovascular Regeneration, University of Frankfurt am Main, Frankfurt am Main 60590, Germany; ‡Illumina, Inc., San Diego, CA 92122; §Institute of Pathology, University of Heidelberg, Heidelberg 69120, Germany; ¶Department of Vascular Surgery, University of Heidelberg, Heidelberg 69120, Germany; ‖Department of Endovascular Surgery, University of Heidelberg, Heidelberg 69120, Germany; #Department of Cardiology, SLK-Hospital Heilbronn, Bad Friedrichshall 74177, Germany; **Institute of Immunology, University of Heidelberg, Heidelberg 69120, Germany; and ††German Centre for Cardiovascular Research, Partner Site, Heidelberg 69120, Germany

Received for publication February 3, 2014. Accepted for publication August 19, 2014.

This work was supported by the German Research Foundation (ER 682/2-1 to C.E. and DFG SFB938/TP Z2 to F.L.), the German Heart Foundation/German Foundation of Heart Research (to C.E.), the German Academic Exchange Service Heidelberg (to L.Z.), the Goethe University Frankfurt (to K.S.), the German Centre for Cardiovascular Research (to H.A.K.), and the German Ministry of Education and Research (to H.A.K.).

The microarray data presented in this article have been submitted to the Gene Expression Omnibus (http://www.ncbi.nlm.nih.gov/geo/query/acc.cgi?acc=GSE60824) under accession number GSE60824.

Address correspondence and reprint requests to Dr. Christian Erbel, Department of Cardiology, Angiology and Pneumology, Medical Hospital III, University Hospital Heidelberg, INF 410, 69120 Heidelberg, Germany. E-mail address: Christian.Erbel@med.uni-heidelberg.de

The online version of this article contains supplemental material.

Abbreviations used in this article: $Apoe^{-/-}$, apolipoprotein E–deficient; CTGF, connective tissue growth factor; DC, dendritic cell; FDR, false discovery rate; GSEA, gene set enrichment analysis; iNOS, inducible NO synthase; LDL, low-density lipoprotein; LPE, local pooled error; oxLDL, oxidized low-density lipoprotein.

University of Heidelberg. Mice were fed a normal chow diet. A total of 100 μg blocking mouse IgG1 anti–IL-17A mAb, kindly provided by F. Di Padova (3-784-9; Novartis Institutes for BioMedical Research) ($n = 15$), or of isotype IgG1 ($n = 10$) was administered i.p. once a week for 16 wk. In addition, 26-wk-old Apoe$^{-/-}$ mice ($n = 5$) were used to quantify lesion area at baseline. Housing and care of animals and all procedures were performed in accordance with the guidelines and regulations of the local Animal Care Committee (Institutional Review Board approval AZ G-41/08).

Tissue processing

For RNA isolation, aortic arches were dissected and snap-frozen as described previously (7). We calculated the cross sectional area by taking the mean surface area of the lesion of each section of each mouse (μm^2). The fractional stenosis was calculated by dividing the surface of the lesion area by the surface of the vessel (including plaque area) and multiplied by 100 (%). The maximum stenosis was analyzed by dividing the vessel area including the lesion area by the vessel area without the lesion area of the section with the highest grade of stenosis of each mice and multiplied by 100 (%).

Quantification of atherosclerotic lesions in the aortic root

After sacrifice, mice were perfused by cardiac puncture with 0.9% NaCl. Afterwards, aortic root was dissected, embedded in OCT, and stored at −20°C. For immunohistochemistry, the aortic root was serially sectioned in 5-μm sections. A section was stained every 75 μm in the direction of the aortic arch with Oil Red O and hemalaune, beginning from the point at which all three aortic valve leaflets first appeared. Routinely, approximately eight consecutive histological sections per mice, taken every 75 μm and covering the root of the aorta, were used to analyze the atherosclerotic lesion and the vessel area. All stainings were captured under identical lighting, microscope, camera, and PC conditions and stored as TIFFs. Slides were analyzed using a Nikon Eclipse TE 2000-E inverted system microscope connected to a Hewlett Packard computer with NIS-Elements AR 2.30 software (Nikon, Duesseldorf, Germany).

For morphometric analysis of the fibrous cap, the thickness was measured in six parts of the cap. The mean thickness of the fibrous cap was calculated for each section of each mice and compared between groups.

Immunohistochemistry and Movat pentachrome staining

Briefly, after fixation in acetone primary Abs against the following Ags were used and titrated to optimum performance: CD3, VCAM-1 (both BD Pharmingen), CD11c (eBioscience), α-smooth muscle actin (Dianova), CD206 (AbD Serotec), Mac-2 (Accurate Chemie), and B220 (Affymetrix). Isotype- and concentration-matched rat control mAb served as negative controls. Biotinylated goat anti-rat IgG (Jackson ImmunoResearch Laboratories) was used as a secondary reagent (1/100, 30 min at room temperature). For plaque composition analyses, Movat pentachrome staining was performed. A thresholding technique using computerized ImagePro analysis was implemented for analysis of the aortic root sections.

Determination of plasma lipid concentration and plasma cell composition

Total serum cholesterol, high-density lipoprotein, low-density lipoprotein (LDL) cholesterol, triglycerides, and blood counts were analyzed by the department of clinical chemistry of the University of Heidelberg.

Real-time PCR

The RNeasy kit (Qiagen), cDNA kit (Roche Diagnostics), and Roche real-time PCR kit with SYBR Green (Roche Diagnostics) were used as described previously (7). Primer sequences are shown in Table I.

ELISA

Protein expression was measured in the supernatant of the ex vivo model as well as RANTES and GM-CSF in the serum of all mice (42 wk) using appropriate ELISAs (SABiosciences) according to the manufacturers' instructions.

Flow cytometry

For flow cytometry, macrophages were harvested by gentle cell scraping and labeled with the appropriate Abs (CD68, CD36, CD206, inducible NO synthase [iNOS], CD11b, CD14, CD16, CXCL6, and CXCL1; BD Pharmingen) as described previously (7).

Stimulation of explanted human atherosclerotic plaque tissue

Twelve soft lipid-rich human carotid artery plaques from patients undergoing endarterectomy were obtained. Plaque tissues were cut into small pieces (3 mm), randomly distributed into wells of a 48-well plate, and cultured in RPMI 1640 medium at 37°C in humidified air containing 5% CO_2. Tissue fragments of the same patient were stimulated with 10ng/ml IL-17A, 1 μg/ml LPS, 10 ng/ml IFN-γ, and 5 ng/ml TNF-α alone or in combination for 3 and 8 h, respectively. Unstimulated plaque pieces of the same patient's probe served as controls.

Adhesion of human platelets and monocytes to endothelial cells under dynamic conditions

HUVECs were isolated as described previously (7). Adhesion experiments were performed as described previously (14).

Human macrophage polarization and gene chip experiments

For macrophage polarization, monocyte-derived macrophages were stimulated with 10 ng/ml IL-17A for 18 h. Unstimulated macrophages served as control. After 18 h RNA was isolated from macrophages using columns including a DNAse-step followed by reverse transcription. RNA was labeled and hybridized to Illumina expression profiling for whole genome BeadChipSentrix array (kindly provided by Hudler, German Cancer Research Center). For blood withdrawal, patients gave written consent, and the study was approved by the local institutional ethics committee.

Effects of IL-17A on macrophage differentiation

Human monocyte-derived macrophages were generated. To investigate the impact of IL-17A on macrophage differentiation, isolated monocytes were incubated either with 100 ng/ml rhM-CSF or with 10 ng/ml IL-17A or both for 6 d. After 6 d for macrophage differentiation, RNA was either isolated from macrophages using columns including a DNAse-step followed by reverse transcription (all reagents from Qiagen), or cells were harvested for flow cytometry analysis.

Effects of IL-17A on macrophage/dendritic cell–mediated T cell activation

PBMCs were isolated from peripheral blood as described above. $CD4^+$ T cells were isolated by positive selection according to the manufacturer's instructions (Miltenyi Biotec). For dendritic cell (DC) differentiation, isolated monocytes were incubated in X-Vivo 15 (BioWhittaker) supplemented with 1.5% inactivated human plasma and 10 μl/ml penicillin/streptomycin at 37°C in a humidified air containing 5% CO_2. The cells were stimulated with 200 U/ml GM-CSF (ImmunoTools) and 1000 U/ml IL-4 (ImmunoTools). One milliliter medium supplemented with 400 U/ml GM-CSF and 1000 U/ml IL-4 was exchanged on day 3 and 5.

For T cell activation assays, macrophages or DCs were incubated in 96-well round-bottom plates in RPMI 1640 supplemented with 10% FCS and stimulated with 20 μg/ml oxidized LDL (oxLDL; Sanbio), 100 ng/ml IL-17A (R&D Systems), or oxLDL in combination with IL-17A for 6 h. As a negative control, RPMI 1640 was used. After 6-h preincubation, $CD4^+$ T-cells were added in a ratio of 1:5 and stimulated for 8 and 18 h. After stimulation, T cells were pooled and resuspended in 400 μl MagNA Pure Lyse-Buffer (Roche) with 10 mg/ml DTT (Roche). Subsequently, RNA was isolated and used for cDNA synthesis.

OxLDL-induced foam cell formation

For the oxLDL uptake assay, macrophages were exposed to 10 μg/ml DiI-labeled oxLDL (Hycultec) (in addition to 10 ng/ml IL-17A) for 4 h at 37°C. Subsequently, cells were washed, and fluorescence intensity was assessed by flow cytometry (FACSCalibur; BD Biosciences). Untreated macrophages served as negative controls.

For the foam cell formation assay, macrophages were exposed to 10–20 μg/ml oxLDL (Hycultec) (in addition to IL-17A) for 24 h at 37°C. After washing the cells, we performed an Oil Red O staining. For the Oil Red O staining analysis, we used ImageJ and the plugin color deconvolution for ImageJ (National Institutes of Health). We measured the positive stained area in relation to the area of the cells ($n = 50$) for each group. Untreated macrophages served as negative controls.

Gene chip data analysis

Local pooled error test. For statistical analysis, the open source statistical software package R (www.r-project.org) was used including the local pooled error (LPE) test for differential expression discovery between two conditions (15). Gene chip data were analyzed as described previously (16). Nonexpressed genes were excluded, followed by normalization of data and log2 transformation to achieve normal distribution. A false discovery rate (FDR) to discover probe sets differentially expressed with FDR <0.05 (17). Heat maps were constructed using R in a way that allows

all conditions and genes to freely cluster both in the *x*- (condition) and *y*-axes (gene).

Gene set enrichment analysis. Gene set enrichment was analyzed using an open-access software for gene set enrichment analysis (GSEA) (18) to assess possible similarities between the IL-17A–induced gene expression profile and the known M1 and M2 signatures. The latter were extracted from the gene expression data of monocyte–macrophage differentiation and polarization as published by Martinez et al. (19) (Gene Expression Omnibus data set 2430). Using the LPE test, genes differentially expressed between the M1 and M2 data set were identified and used as M1 and M2 gene sets, respectively. Overexpression of the M1 and M2 gene sets was tested by GSEA in the unstimulated and IL-17A gene expression data. GSEA calculates an enrichment score, which indicates the degree of overrepresentation of these gene sets, and estimates its significance with adjustment for multiple hypothesis testing.

Modified principal component analysis and hierarchical clustering. A modified principal component analysis was performed on the previously published M1 and M2 (19) as well as on the new IL-17A gene expression data normalized to the unstimulated gene expression sets as described previously (20). Briefly, a normalization step was used to avoid bias owing to interexperimental variance. Principal component analysis was performed including all genes that were significantly overexpressed (as determined by LPE) in M1 relative to M2 and all genes that were overexpressed in M2 relative to M1. The first principal components from each of these analyses (independent by definition) were used to define a new coordinate space in which IL-17A gene expression data were plotted. Hierarchical clustering was used to determine the level of similarity between the three normalized groups (21). All genes were included in the analysis, and the results are displayed in a dendrogram.

Microarray data has been submitted to the Gene Expression Omnibus database under accession number GSE60824 (http://www.ncbi.nlm.nih.gov/geo/query/acc.cgi?acc=GSE60824).

Statistical analysis

Figure data are presented as mean ± SEM and tables as mean ± SD. To compare groups of animals, one-way ANOVA (Kruskal-Wallis) was used to compare the groups. Significant differences with $p \leq 0.05$ or weak differences with $p < 0.1$ were specified using Mann–Whitney *U* or *t* test, where indicated. For adhesion assays, ANOVA test with Scheffe post hoc analysis was applied to determine significant differences between groups. A p value < 0.05 was considered statistically significant.

Table I. Primer sequences

Name	Sequence
mIFNγ FP	5′-ATGAACGCTACACACTGCATC-3′
mIFNγ RP	5′-CCATCCTTTTGCCAGTTCCTC-3′
mIL4 FP	5′-ACTTGAGAGAGATCATCGGCA-3′
mIL4 RP	5′-AGCTCCATGAGAACACTAGAGTT-3′
mIL6 FP	5′-TAGTCCTTCCTACCCCAATTTCC-3′
mIL6 RP	5′-TTGGTCCTTAGCCACTCCTTC-3′
mLCK FP	5′-TGGAGAACATTGACGTGTGTG-3′
mLCK RP	5′-ATCCCTCATAGGTGACCAGTG-3′
mCCL2 FP	5′-TTAAAAACCTGGATCGGAACCAA-3′
mCCL2 RP	5′-GCATTAGCTTCAGATTTACGGGT-3′
mTNFα FP	5′-CCCTCACACTCAGATCATCTTCT-3′
mTNFα RP	5′-TGCTACGACGTGGGCTACAG-3′
mIL21 FP	5′-GGA CCC TTG TCT GTC TGG TAG-3′
mIL-21 RP	5′-TGT GGA GCT GAT AGA AGT TCA GG-3′
mIL22 FP	5′-AAC TTC CAG CAG CCG TAC AT-3′
mIL-22 RP	5′-GTA GGG CTG GAA CCT GTC TG-3′
mCCL5 FP	5′-GCT GCT TTG CCT ACC TCT CC-3′
mCCL5 RP	5′-TCG AGT GAC AAA CAC TGC-3′
mCCL20 FP	5′-CCA GTT CTG CTT TGG ATC AGC-3′
mCCL20 RP	5′-GCC TCT CGT ACA TAC AGA CGC-3′
hICAM1 FP	5′-GGCCTTATTCCTCCCTTCC-3′
hICAM1 RP	5′-GGCATAGCTTGGGCATATTC-3′
hIL6 FP	5′-AAATTCGGTACATCCTCGACGG-3′
hIL6 RP	5′-GGAAGGTTCAGGTTGTTTTCTGC-3′
hCCL2 FP	5′-ATGAAAGTCTCTGCCGCCCTTCT-3′
hCCL2 RP	5′-TGAGTGTTCAAGTCTTCGGAGTT-3′
hTF FP	5′-TACTTGGCACGGGTCTTCTC-3′
hTF RP	5′-TCACATTCACTTTTGTTCCCA-3′
hTNFα FP	5′-TCTTCTCGAACCCCGAGTGA-3′
hTNFα RP	5′-CCTCTGATGGCACCACCAG-3′
hIFNγ FP	5′-TCGGTAACTGACTTGAATGTCCA-3′
hIFNγ RP	5′-TCCTTTTTCGCTTCCCTGTTTT-3′
hMMP9 FP	5′-TGGCAGAGATGCGTGGAGA-3′
hMMP9 RP	5′-GGCAAGTCTTCCGAGTAGTTTT-3′
hCol1.2 FP[a]	5′-AAC CAA GGA TGC ACT ATG GA-3′
hColl1.2 RP[a]	5′-GCT GCC AGC ATT GAT AGT TT-3′

Primer sequences (murine [m] and human [h]), forward primer (FP), and reverse (RP) primer are shown.
[a]Obtained from Biomol (Hamburg, Germany).

Results

Experimental study group

Based on previous dose-finding studies (7), mice in the therapy group were treated with 100 μg anti–IL-17A mAb by i.p. injection once a week for 16 wk. The Mab 3-784-9 was previously shown to be sufficient to deplete IL-17A in vivo (22). Primer sequences for the quantitative tissue PCR analysis of the thoracic aortae of mice are presented in Table I. No animal died, and no growth retardation (body weight and height) was observed. At 42 wk of age, serum concentrations of total cholesterol, high-density lipoprotein and LDL cholesterol, triglycerides, and whole blood counts did not differ between both groups (Table II).

IL-17A mAb treatment attenuated progression of advanced atherosclerotic lesions in Apoe$^{-/-}$ mice

Fig. 1A–C shows histology of representative aortic root sections of the different groups. IL-17A mAb treatment prevented lesion progression with a cross-sectional area of 471,359 ± 42,650 μm^2 (mean ± SEM) versus 721,989 ± 78,099 μm^2 in control mice (−35%; $p = 0.01$, Fig. 1D). Fractional and maximum stenosis were also markedly reduced in IL-17A mAb–treated as compared with control mice (fractional stenosis: −39%; 26.9 ± 7 versus 44.1 ± 8%; $p = 0.001$; Fig. 1E; maximum stenosis: −29%; 35.15 ± 8 versus 49.71 ± 9%; $p = 0.001$; Fig. 1F). When compared with atherosclerotic lesion formation at baseline (26-wk-old mice), IL-17A blockade also significantly reversed fractional stenosis (−43%, $p = 0.01$; Fig. 1E).

By Movat pentachrome staining, we found that IL-17A inhibition significantly reduced the necrotic core in atherosclerotic plaques compared with control mice ($p = 0.007$; control, 38,113 ± 22,001 versus therapy, 22,546 ± 11,080 μm^2; data not shown). Accordingly, plaque cellularity was significantly lower in the treatment versus control group ($p = 0.01$; control, 897 ± 255, versus therapy, 608 ± 202; data not shown).

IL-17A mAb treatment increased plaque stability in Apoe$^{-/-}$ mice

Anti–IL-17A mAb treatment resulted in significantly thicker fibrous caps compared with controls ($p = 0.008$; Fig. 2A, 2B). In addition, Movat staining showed that IL-17A mAb–treated mice displayed markedly higher amounts of lesional collagen than controls (66%; 32.66 ± 8 versus 49.24 ± 14%; $p = 0.01$; Fig. 2A, 2B). The results of the collagen content in the lesion were confirmed by two-photon confocal microscopy. Treatment with anti–IL-17 mAb resulted in a significant increase of the collagen content in the plaques compared with controls ($p = 0.02$, Fig. 2A, 2B). These findings were supported by the significantly increased mRNA expression of connective tissue growth factor (*CTGF*), which is involved in the fibrosis cascade, in IL-17A mAb–treated versus control mice ($p = 0.04$; Table III). Total numbers of smooth muscle cells did not differ between the groups (Fig. 2A, 2B). Although apoptotic cell death by TUNEL staining was found in both groups, the amount of TUNEL$^+$ cells in atherosclerotic lesions was significantly lower in the therapy group ($p = 0.03$; Fig. 2A, 2B).

Table II. Blood and baseline parameters

Parameter	Baseline (± SD) (n = 5)	Control (± SD) (n = 10)	IL-17 mAb (± SD) (n = 15)	p Value
Leukocytes (nl)	4.51 ± 3	4.04 ± 2	4.97 ± 2	NS
Erythrocytes (pl)	6.73 ± 2	6.02 ± 1	6.98 ± 1	NS
Hemoglobin (g/dl)	10.55 ± 3	9.58 ± 2	11.28 ± 1	NS
Thrombocytes (nl)	577.40 ± 587	581.10 ± 300	553.10 ± 459	NS
Triglycerides (mg/dl)	80.47 ± 124	98.50 ± 100	67.73 ± 38	NS
Total cholesterol (mg/dl)	203.82 ± 122	201.00 ± 158	195.91 ± 129	NS
LDL cholesterol (mg/dl)	208.76 ± 163	216.87 ± 127	196.0 ± 115	NS
Body weight (g)	32.11 ± 5	37.8 ± 5	33.16 ± 4	NS
Height (cm)	9.0 ± 1	9.3 ± 0.6	9.18 ± 0.5	NS

Body weight and height, lipid profile, and hematological parameters were measured on the day of tissue harvesting (42 wk) of IL-17 mAb–treated mice and controls.

Reduced lesional cellular infiltration and activation in anti–IL-17A mAb–treated mice

Immunohistochemistry revealed a significant reduction of $CD3^+$ T cells ($p = 0.01$) and T cell density ($p = 0.04$) in atherosclerotic lesions of anti–IL-17A mAb–treated mice compared with control mice (Fig. 3A, 3B). No differences were found between groups for mRNA expression of *LCK* (lymphocyte-specific protein tyrosine kinase, a marker of the CD4 TCR), the Th2 cytokine *IL4*, and the T cell activation marker *IFNγ* (Table III).

Lesional Mac-2^+ macrophages were reduced both in total number and numbers per lesion in IL-17A mAb–treated compared with control mice ($p = 0.02$ and $p = 0.04$, respectively; Fig. 3A, 3B). The proportion of monocyte-originated cells, including anti-inflammatory M2 macrophages, identified by Mac-2 and CD206 staining, was similar between the groups (NS; Fig. 3A, 3B). mRNA levels of the most potent macrophage chemoattractant *CCL2* were significantly reduced in IL-17A mAb–treated mice ($p = 0.02$; Table III). Also, the grade of activation of macrophages as determined by *TNFα* mRNA expression was significantly reduced compared with control mice ($p = 0.03$; Table III).

In the baseline group, mean density of $CD3^+$ T cells was 0.08 ± 0.009 (mean ± SD) and MAC-2^+ area 28,371 ± 17,623 μm^2 in atherosclerotic lesions (Fig. 3).

B cell numbers did not differ significantly between groups ($p = 0.05$; controls [mean ± SD], 0.9 ± 1.1, versus therapy, 3.0 ± 2.8; Fig. 3A, 3B).

Protein serum levels of RANTES and GM-CSF were significantly reduced in anti–IL-17A mAb–treated mice compared with controls (both $p = 0.04$; data not shown).

Effects of endothelial IL-17A stimulation on monocyte and platelet adhesion and platelet rolling

Monocyte adhesion was significantly increased after IL-17A stimulation compared with resting endothelial cells (all $p < 0.05$; Fig. 4A). Because platelet adherence by IL-17A may support the recruitment of circulating monocytes, we also investigated rolling and firm adhesion of perfused platelets on IL-17A–stimulated HUVECs and found both to be increased under high shear conditions (versus unstimulated, all $p < 0.05$; Supplemental Fig. 1). Representative videos of endothelial cell–adherent platelets are shown in Supplemental Videos 1–3.

IL-17A does not affect monocyte-derived macrophage differentiation

Incubation of monocytes with IL-17A for 6 d did not affect macrophage differentiation at the gene expression (data not shown) or protein level (Table IV) compared with M-CSF.

IL-17A induces a proinflammatory transcriptome in macrophages

The effects of IL-17A on macrophage differentiation and transcriptomes were analyzed after treatment with recombinant human IL-17A (10 ng/ml) or control for 18 h. The 222 probe sets were significantly regulated by LPE test (FDR < 0.05; 162 up- and 60 downregulated) (Fig. 4B). A substantial number of proinflammatory mediators were upregulated, including cytokines such as *IL1A* and *IL6* or chemokines like *CCL2*, *CCL8*, *CCL20*, *CXCL1*, *CXCL2*, and *CXCL6*. Furthermore, genes involved in oxidative stress were induced, including several metallothioneines (*MT1M* and *MTE*). Also, genes coding for surface receptors such as *CD14*, *CD163*, or *TLR8* were significantly upregulated. By contrast, IL-17A at the same time induced downregulation of several genes implicated in T cell costimulation, including *CD40* and *CD83* (Fig. 4C).

We compared the IL-17A–induced macrophage transcriptome with established macrophage polarization types using previously identified gene sets for M1 (LPS/IFN-γ), M2 (IL-4) (19), and M4 (CXCL4) macrophages (20). Although the M2 and M4 gene sets were not significantly enriched, we found a significant overexpression of the M1 gene set consistent with the proinflammatory role of IL-17A and M1 macrophages (Fig. 4D, 4E). Using the entire transcriptomes of M1, M2, and M4 macrophages normalized to their M-CSF–treated counterparts and performing hierarchical clustering, IL-17A–treated macrophages were distinct from any other macrophage polarization type (Fig. 4D, 4E).

IL-17A does not affect lipid uptake and macrophage foam cell formation

To assess a possible additive effect of IL-17A and oxLDL on DC- and macrophage-dependent activation of T cells, we studied oxLDL uptake and macrophage foam cell formation. Oil Red O staining did not reveal changes in oxLDL uptake after 24-h incubation with IL-17A or control (Fig. 5A, 5B). Similarly, flow cytometry did not show any changes of DiI-oxLDL uptake in macrophages treated with IL-17A or control (Fig. 5C).

IL-17A induces proinflammatory mediators in cocultures of oxLDL-treated macrophages or DCs with $CD4^+$ T cells

oxLDL is a potent autoantigen and, like LPS, binds to TLR4 (23). If macrophages were primed with oxLDL for 6 h before coculture with $CD4^+$ T cells, T cell proliferation genes were significantly upregulated as compared with cocultures with untreated macrophages or T cells alone (8 h in Fig. 5D; 18 h, not shown). Addition of 100 ng/ml IL-17A to cocultures induced marked mRNA upregulation of genes attributed to the Th1 cell linage (*T-box21*

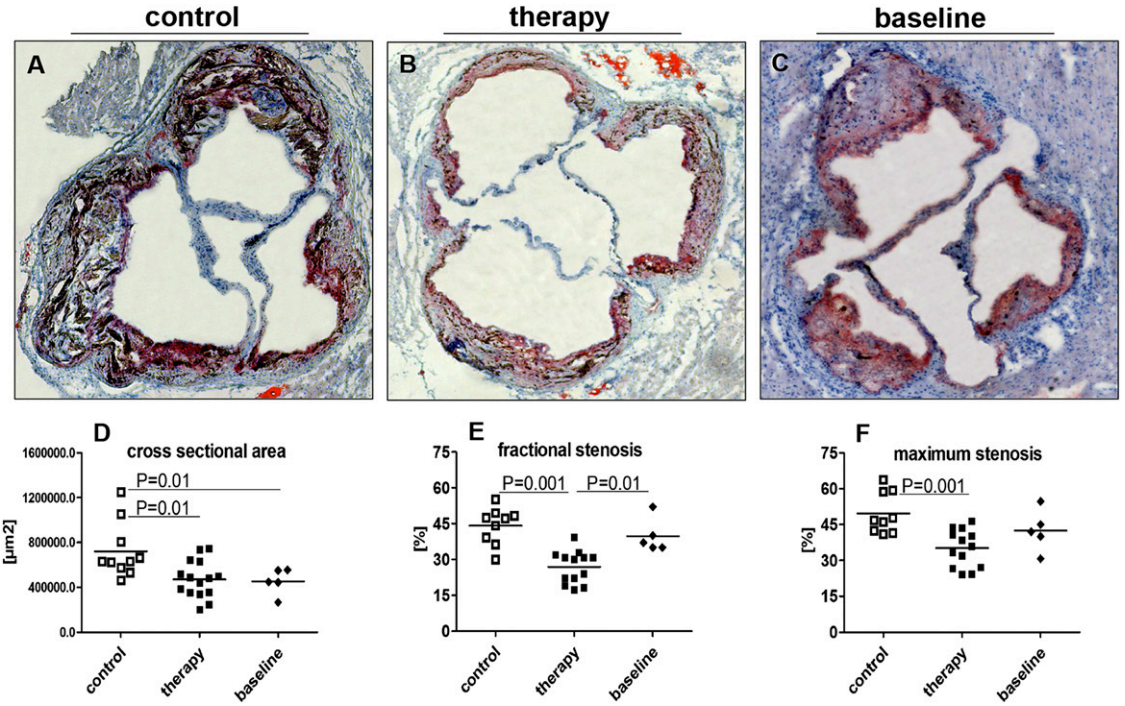

FIGURE 1. Effects of IL-17A mAb treatment on atherosclerotic plaques in Apoe$^{-/-}$ mice. Representative Oil Red O immunohistostainings (original magnification ×4) from aortic root of control [n = 10; (**A**)]; IL-17A mAb-treated mice [n = 15; (**B**)] and baseline [n = 5; (**C**)] are shown. (**D**–**F**) Morphometric quantification of cross-sectional area (µm^2), fractional stenosis (%), and maximum stenosis (%) of late-stage atherosclerotic lesions were compared. Results are shown as dot plots displaying mean.

[T-bet]) or genes associated with T cell activation (*IL2* and *IFNγ*, Fig. 5D; *CD40L*, data not shown). Furthermore, genes coding for cytokines of the IL-17A pathway (*IL21* and *IL27*) and *IL10*, but not *FOXP3* were upregulated after 8 h and also to a lesser degree at 18 h (data not shown). No change was seen for the Th2 lineage genes *GATA3* (data not shown) and *IL4* (data not shown). DCs showed a mark higher grade of activation than macrophages; only the transcription factors *FOXP3* and *GATA3* displayed higher expression levels in T cells, cocultured with macrophages (data not shown).

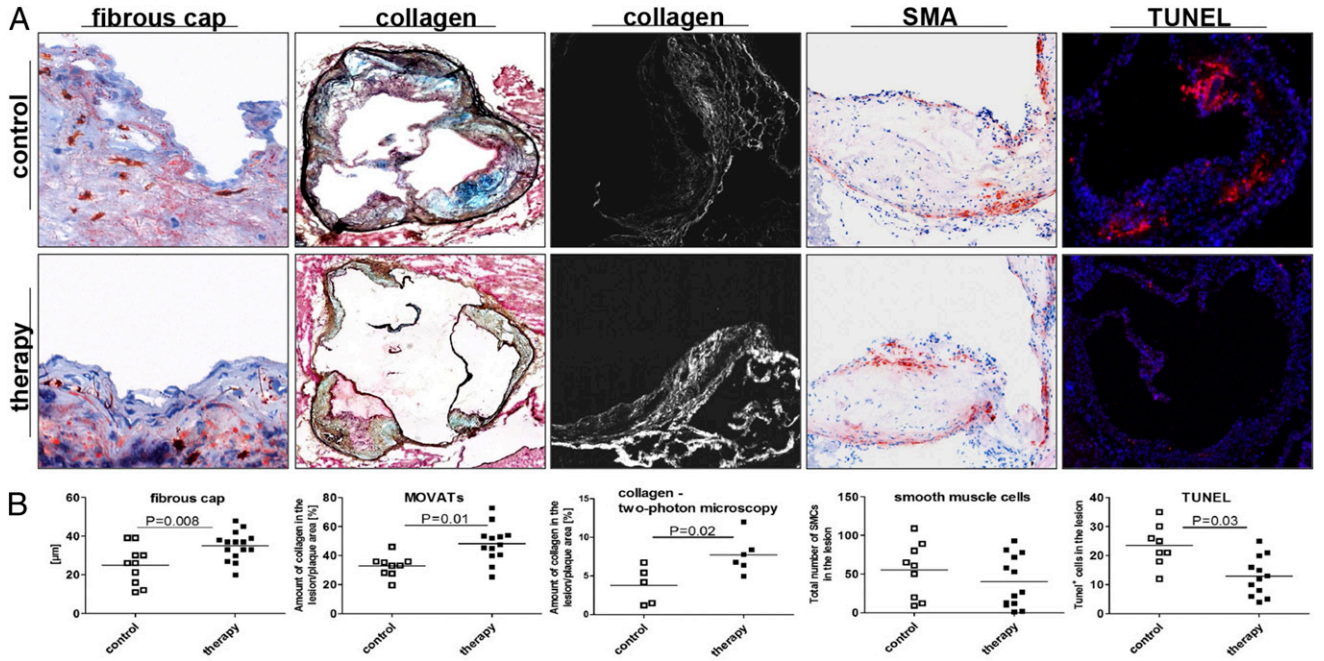

FIGURE 2. Plaque morphology of the aortic root of Apoe$^{-/-}$ mice. (**A**) Plaque stability was assessed by quantification of the fibrous cap (µm), collagen content per plaque area (Movat pentachrome staining, original magnification ×4, and two-photon microscopy, original magnification ×40) as well as total number of smooth muscle cells (SMA; original magnification ×40) and apoptotic cells (TUNEL; original magnification ×4) in the lesion. (**B**) Quantitative analysis of lesion composition of IL-17A mAb–treated (n = 12–15) and control animals (n = 8–10). Results are presented as dot plots displaying mean.

Table III. Quantitative tissue PCR results for different cytokines, chemokines, CTGF, and kinase LCK from the thoracic aorta

Variable	Control ΔC_T ($\pm$ SD) (n = 10)	IL-17 mAb-Treated ΔC_T ($\pm$ SD) (n = 15)	p Value
IL4	346.71 $\pm$ 292	308.91 $\pm$ 199	NS
IL6	161.9 $\pm$ 83	100.8 $\pm$ 46	0.04
IL21	29.66 $\pm$ 17	27.75 $\pm$ 8	NS
IL22	214.65 $\pm$ 97	226.69 $\pm$ 82	NS
IFNγ	70.02 $\pm$ 31.14	115.5 $\pm$ 96.12	NS
TNFα	51.02 $\pm$ 26	42.15 $\pm$ 15	0.03
CCL2 (MCP-1)	257.75 $\pm$ 94	210.60 $\pm$ 50	0.02
CCL20 (MIP-3α)	116.74 $\pm$ 73	112.22 $\pm$ 44	NS
CTGF	80.29 $\pm$ 80.29	138.0 $\pm$ 69.54	0.04
LCK	53.00 $\pm$ 34	47.69 $\pm$ 19	NS

Data are normalized to β-actin and expressed as cDNA copies/1000 β-actin copies.

Proinflammatory and plaque-destabilizing effects in IL-17A–stimulated human atherosclerotic lesions

To address the effects of IL-17A on human atherosclerotic lesions, we exposed plaque cultures to rIL-17A. Treatment with IL-17A induced mRNA upregulation of various proinflammatory mediators after 3 and 8 h (Fig. 6A, 6B), including the chemokine MCP-1 (*CCL2*) (p = 0.0006 after 8 h) and the plaque-destabilizing matrix metalloprotease *MMP9* (p = 0.01 after 8 h; Fig. 6A). In addition, IL-17A induced mRNA expression of the proinflammatory cytokine *TNFα* (p = 0.01 after 3 h and p = 0.004 after 8 h) and the adhesion molecule *ICAM1* ($p < 0.005$ after 3 h and p = 0.01 after 8 h) and *IL6* (p = 0.002 after 8 h; Fig. 6B). By analyzing the mRNA levels of collagen type 1, we found a significant downregulation in the therapy versus control group (p = 0.007; Fig. 6A).

IL-17A–induced effects were even more pronounced at the protein level (Table V). IL-6, TNF-α, G-CSF, and TGF-β were significantly upregulated in supernatant, whereas IFN-γ was unchanged (Table V).

To confirm the in vitro effects of IL-17A on macrophage polarization ex vivo, we measured molecules predominantly expressed by IL-17A–polarized macrophages and found increased *CXCL1* (p = 0.03; Fig. 6A), *CXCL2*, and *CXCL6* (both p = 0.04) mRNA expression levels after 3 and 8 h (data not shown).

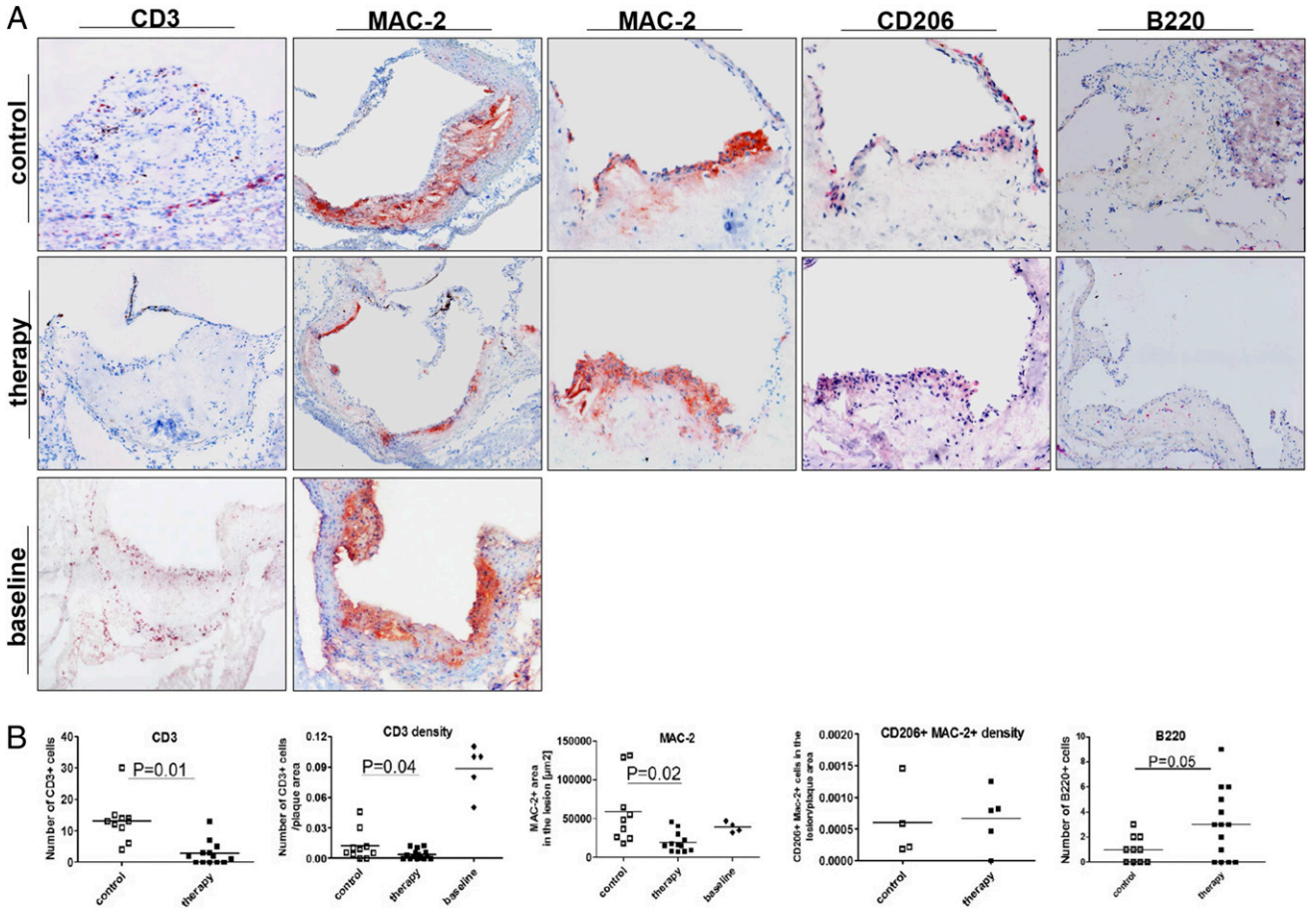

FIGURE 3. Cellular composition in atherosclerotic lesions of Apoe$^{-/-}$ mice. (**A**) Representative photomicrographs of immunohistochemistry stainings of T cells (CD3, original magnification ×40), Mac-2$^+$ cells (original magnification ×40), CD206$^+$ cells (original magnification ×40), and B cells (B220; original magnification ×40). (**B**) Quantitative analysis of plaque inflammation are presented in 42-wk-old Apoe$^{-/-}$ mice with (n = 12–15) and without IL-17A mAb treatment (n = 8–10) (as well as 26-wk-old baseline mice, n = 4 to 5). Results are presented as dot plots displaying mean.

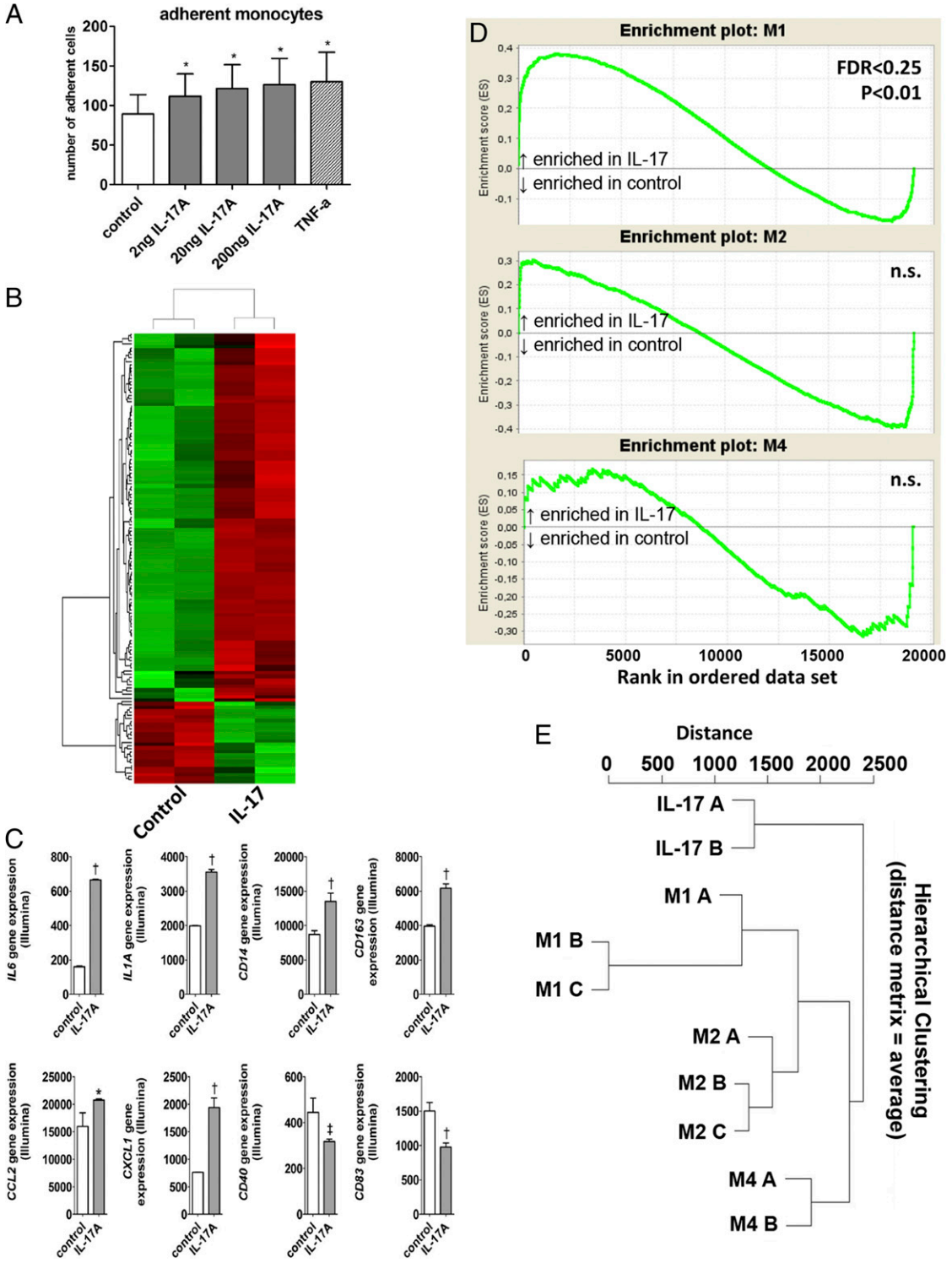

FIGURE 4. IL-17A polarizes macrophages toward a distinct proinflammatory transcriptome. (**A**) Adhesion of monocytes to endothelial cells under static conditions. HUVEC monolayers were pretreated with IL-17A or TNF-α, and monocytes were added for additional 30 min at 37˚C in a humidified 5% CO_2/95% air mixture. Nonadherent cells were removed by washing twice with PBS. Adherent monocytes were quantitated by direct phase-contrast microscopy. Mean ± SEM of nine independent static adhesion assay experiments. *Versus unstimulated HUVECs, all $p < 0.05$. (**B**) Heat map of genes regulated by IL-17A (10 ng/ml for 18 h) as determined by LPE analysis (FDR < 0.05). (**C**) Expression of selected proinflammatory cytokines, chemokines, surface receptors, and costimulatory molecules significantly regulated by IL-17A (*$p < 0.05$, $^{\dagger}p < 0.01$, $^{\ddagger}p < 0.001$). (**D**) GSEA assessing overexpression of predefined gene sets based on transcriptomic analyses of M1 (LPS and IFN-γ), M2 (IL-4), or M4 (CXCL4) macrophages. (**E**) Hierarchical clustering of IL-17A–treated macrophages and M1 (LPS and IFN-γ), M2 (IL-4), or M4 (CXCL4) macrophages.

Synergistic effects of IL-17A in addition to LPS in the plaque microenvironment

In the presence of LPS, IL-17A stimulation induced >5-fold higher *TNFα* mRNA expression and 55% higher *ICAM1* mRNA expression compared with IL-17A alone (Fig. 6B). No synergistic effect of IL-17A and LPS was seen for *IL6* (Fig. 6B), *IFNγ*, *TF*, MCP-1 (*CCL2*), and *MMP9* (data not shown). Interestingly, no additive effects were seen for IL-17A in addition to TNF-α and IFN-γ (Supplemental Fig. 2).

Table IV. Flow cytometry results for monocyte-derived macrophage differentiation in vitro

Parameter	Unstimulated Percent Total	IL-17 Percent Total	M-CSF Percent Total	M-CSF + IL-17 Percent Total
CD68/CD36/CD206$^+$	3.93 ± 2.7	4.45 ± 3.7	12.67 ± 9.8	8.31 ± 4.1
CD68/CD36/CD206$^-$	0.40 ± 0.3	0.08 ± 0.04	3.22 ± 2.7	1.41 ± 0.8
CD68/CD36/iNOS$^+$	3.40 ± 2.5	2.00 ± 1.7	8.74 ± 5.6	7.27 ± 6.7
CD68/CD36/iNOS$^-$	0.68 ± 0.9	0.17 ± 0.1	8.18 ± 4.5	3.44 ± 2.4
CD11b/CD14$^+$/CD16$^+$	2.35 ± 1.6	1.13 ± 0.9	12.59 ± 8.3	8.83 ± 6.3
CD11b/CD14$^+$/CD16$^-$	5.28 ± 4.7	1.38 ± 1.0	20.53 ± 11	17.84 ± 13
CD11b/CD14$^-$/CD16$^+$	0.00 ± 0.0	0.02 ± 0.01	0.03 ± 0.01	0.02 ± 0.01

Data are shown as mean ± SD.

Discussion

IL-17A plays a central role in various autoimmune diseases. This has led to IL-17A as a targeted biologic therapy and is currently tested in phase 2 and 3 studies for the treatment of psoriasis and rheumatoid arthritis. Atherosclerosis as a chronic (auto)immune disease is influenced by IL-17A inhibition as well (5, 7, 8, 11).

The current study demonstrates that blocking IL-17A with anti–IL-17A mAb prevents progression of advanced late-stage atherosclerotic lesions in Apoe$^{-/-}$ mice. The underlying mechanisms include reduced inflammatory cellular infiltration (monocyte-originated cells and T cells) with attenuation of tissue activation. In addition, blocking IL-17A resulted in reduced plaque vulnerability. In vitro, IL-17A induces adhesion of human monocytes and adhesion and rolling of platelets on endothelial cells and polarizes macrophages toward a distinct proinflammatory macrophage subtype. IL-17A sensitized human macrophages and DCs, as well as the TLR4 ligand oxLDL in vitro, induced upregulation of proinflammatory, prothrombotic, and plaque-destabilizing molecules in human plaques ex vivo, and potentiated LPS-dependent upregulation of various inflammatory mediators. Thus, IL-17A appears to be an important player in not only murine, but also in human atherosclerosis.

Atherosclerosis and its consequences (i.e., myocardial infarction and stroke) remain the major cause of morbidity and mortality in Western countries. Several studies have investigated the role of IL-17A in the development of atherosclerosis with partially controversial results (7–11, 24–26), which are at least partially based on the study design, neutralizing Ab versus bone marrow transfer experiments, on the type of diet, and on the location of the analysis of the atherosclerotic lesion. By contrast, the current study evaluated the role of IL-17A on advanced atherosclerotic lesions and its potential impact as a therapeutic target. In contrast to early lesions, advanced atherosclerosis is the common disease phenotype in clinical care, as coronary, cerebral, or peripheral artery disease is usually diagnosed at a stage at which lesions have already developed and progressed. As shown, IL-17A mAb treatment prevents the progression of advanced atherosclerotic lesions and induced plaque stability in mice, mainly by downregulating the inflammatory compound. Thus, IL-17A influences not only early, but also advanced atherosclerotic lesions. Notably, the results only refer to the aortic sinus and cannot be transferred to other vessel regions like the innominate artery.

Plaque vulnerability is the initial step to plaque rupture, which is followed by a vessel occlusion, leading to a myocardial infarction or stroke. The role of IL-17A in plaque vulnerability in the early phase of atherosclerosis has been stated by four groups. In vivo, our group and others found that direct inhibition by anti–IL-17A mAb treatment or Apoe$^{-/-}$/IL-17A$^{-/-}$ mice resulted in a stabilization of atherosclerotic plaque (7, 24), whereas indirect inhibition of IL-17A over inhibition of suppressor of cytokine signaling 3 or Smad7 led to plaque vulnerability (10, 11). Okamoto et al. (27) reported that in IL-17A$^{-/-}$ mice, CTGF mRNA expression was reduced, and in vitro, a murine skin fibroblast cell line showed an IL-17A–dependent increase of TGF-β, CTGF, and collagen. The current study supports the hypothesis of IL-17A as a plaque-destabilizing molecule. We found that in progressed atherosclerosis, IL-17A inhibition in Apoe$^{-/-}$ mice leads to marked plaque stability and increases CTGF expression in the thoracic aorta. The underlying reasons of the discrepant results are primarily due to a different type of mice, stage of atherosclerotic lesion progression, and IL-17A inhibitory treatment used in the studies mentioned above. Thus, the current study identifies the impact of IL-17A in plaque vulnerability in late-stage atherosclerosis; however, additional studies are needed to further evaluate the underlying reasons of the controversial results.

Based on the potent effects of IL-17A on murine early and advanced atherosclerotic lesions, we further intended to evaluate the role of IL-17A on human lesions. Previous studies from our group and others have demonstrated expression of IL-17A in human atherosclerotic lesions (11, 12). IL-17A tissue release is more abundant in patients with ischemic symptoms and complicated lesions, but interestingly independent of the standard coronary artery disease medication (13). IL-9, known to facilitate Th17 cell expansion and to stimulate production of IL-17, is increased systemically and locally in patients with carotid and coronary atherosclerosis and increased IL-17 release in PBMCs from patients with unstable angina (28). Focusing on the cellular origin, predominantly macrophages, but also T cells, mast cells, and B cells, express IL-17A (12, 13). Furthermore, a recent study showed that higher numbers of IL-17A– and IFN-γ–expressing T cells are present in peripheral blood of patients with severe myocardial infarction compared with those with stable coronary artery disease. Moreover, cultured lesional human T cells express IL-17A and IFN-γ after polyclonal stimulation compared with T cells extracted from nondiseased vessels (29), and an unstable angina patient presented elevated levels of plasma IL-17A and the Th17-related cytokines IL-6 and IL-23 (30). In contrast, IL-17A induced collagen production by human vascular smooth muscle cells, and retinoic acid–related orphan receptor γt mRNA was associated with collagen type I and α-smooth muscle actin mRNA expression in human atherosclerotic plaques (11). In addition, one clinical study showed that low serum levels of IL-17 might be associated with a higher risk of major cardiovascular events (31). The current study supports the hypothesis of IL-17A to be involved in the inflammatory milieu and plaque instability in atherosclerotic lesions. IL-17A stimulation of human plaque fragments induced a proinflammatory, prothrombotic, plaque-destabilizing, and cell-attracting response. Because of the reported synergistic effects of IL-17A, TNF-α, IFN-γ, and LPS (7, 29, 32), we investigated a possible additive effect on the inflammatory milieu in cultured human carotid plaques. Only IL-17A in addition to LPS showed

additive proinflammatory effects on the plaque microenvironment. Interestingly, the activation of the inflammatory milieu by IL-17A was more substantial than IFN-γ or TNF-α alone. The explanation for the discrepant results might be on the basis of different study protocols, including the type of cells and analytic methods used in the studies listed above. In conclusion, the data clearly identify IL-17A as an independent and effective proinflammatory modulator in human plaque microenvironment that may promote plaque instability and plaque rupture; however, further studies are necessary to evaluate the relevance of the findings in the clinical setting.

Because IL-17A is prominently involved in early and advanced atherosclerotic lesion formations, we further evaluated the underlying mechanisms by analyzing the impact of IL-17A on monocytes and monocyte-derived cells, which are known to play a major role during disease development and progression (4, 33, 34). Previous studies have convincingly shown that migratory egress of monocyte-derived cells is a major step (35), but reduction of monocyte recruitment seems to be even more important in reducing plaque monocyte-originated cells burden (4). We already showed that IL-17A inhibition reduces lesional chemokine expression (*CCL5*) in early atherosclerotic lesions and IL-17A induces expression of adhesion molecules on endothelial cells (VCAM-1) (5, 7). Further analysis was done by Butcher et al. (25) showing a downregulation of various chemokines in IL17A$^{-/-}$ Apoe$^{-/-}$ as well as in IL-17RA$^{-/-}$Apoe$^{-/-}$ mice in early atherosclerotic lesions. The current study demonstrates a downregulation of *CCL2* mRNA transcripts and serum protein level of CCL5 in anti–IL-17A mAb–treated mice in advanced atherosclerotic lesions and the upregulation of various chemokines in IL-17A–polarized macrophages in vitro. Moreover, Butcher et al. (25) found that IL-17RA is involved in monocyte recruitment. The current manuscript underlines the finding by showing that IL-17A directly influenced monocyte adherence. We further show that there is also an indirect pathway to support the recruitment of circulating monocytes by inducing platelet adhesion. Thus, IL-17A is involved in leukocyte recruitment, and this may represent one mechanism by which IL-17A inhibition reduces cellular content and prevents lesion progression.

During atherogenesis, blood monocytes adhere to the activated endothelium, transmigrate into the subendothelial space, and dif-

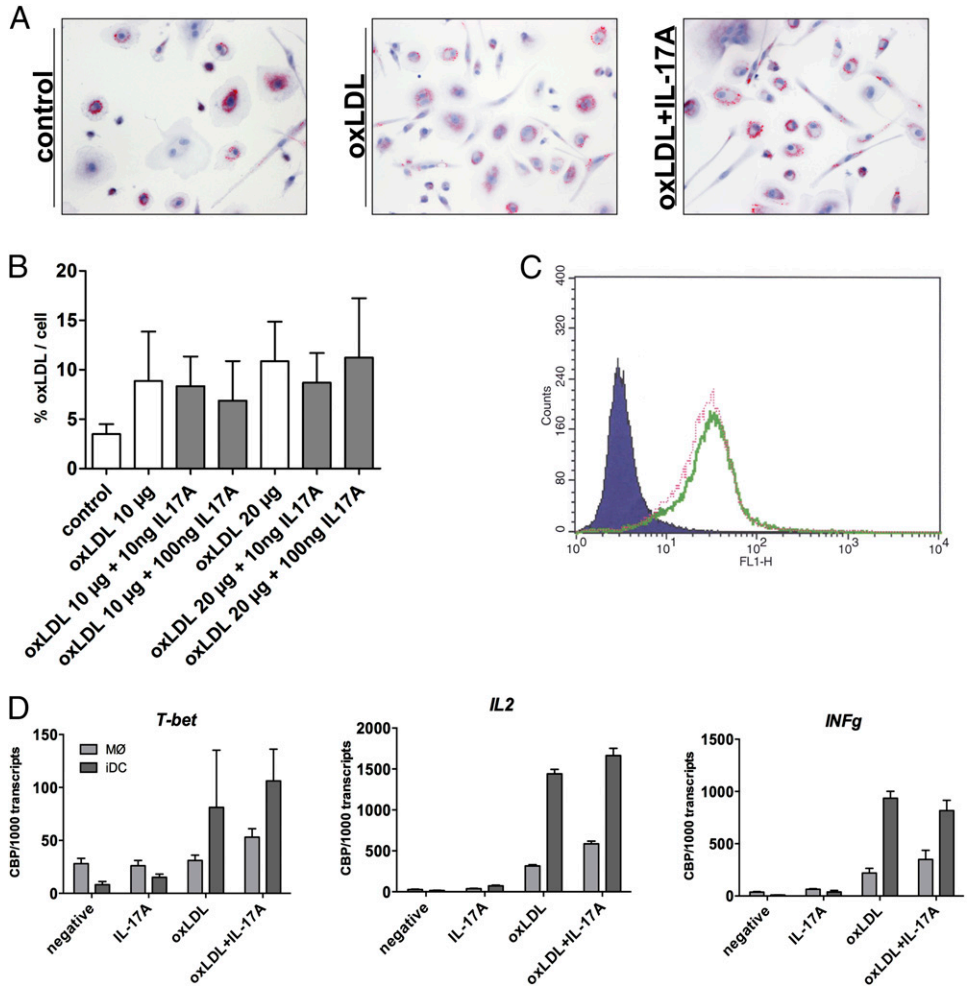

FIGURE 5. Effects of IL-17A on monocytes and monocyte-derived cells. (**A** and **B**) Foam cell formation assay. (A) Representative photomicrographs of monocyte-derived macrophages incubated with oxLDL in addition to IL-17A in different concentrations are shown (original magnification ×20). Representative Oil Red O staining of different groups are shown: no oxLDL (control), oxLDL, and oxLDL plus IL-17A. (B) Data are given as mean ± SEM of five independent experiments. (**C**) oxLDL uptake assay. Flow cytometry analysis of DiI-labeled oxLDL uptake (in addition to IL-17A incubation) of monocyte-derived macrophages: solid green line (oxLDL) and dotted pink line (oxLDL+IL-17A). Histogram represents one out of three independent experiments. (**D**) For T cell activation assays, macrophages or DCs were incubated in 96-well round-bottom plates and stimulated with oxLDL (Sanbio), IL-17A (R&D Systems), or oxLDL in combination with IL-17A. After 6-h preincubation, CD4$^+$ T cells were added in a ratio of 1:5 and stimulated for 8 h. Expression of activation-associated cytokines and transcription factors in CD4$^+$ T cells was measured (see *Materials and Methods* for details). Representative analysis of *T-box21* (T-bet), *IL2*, and *IFNγ* are shown.

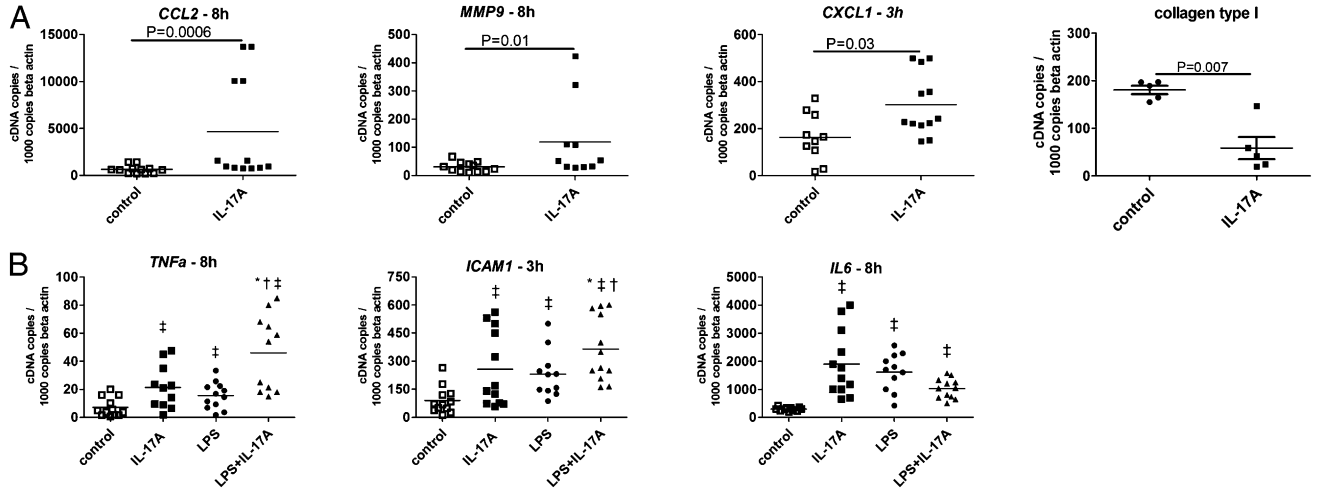

FIGURE 6. (Synergistic) effects of IL-17A stimulation on the inflammatory milieu in human carotid plaque tissues. Pieces of lipid-rich plaque tissue were stimulated with 10 ng/ml IL-17A, LPS (1 μg/ml), TNF-α (5 ng/ml), IFN-γ (10 ng/ml), or combined and compared with an unstimulated part of the plaque (n = 5–12, respectively). Transcripts of MCP-1 (*CCL2*) and *MMP9* after 8 h, *CXCL1* and collagen type 1 after 3 h (**A**), as well as *TNFα* and *IL6* (**B**) after 8 h and *ICAM1* after 3 h (B) were measured by quantitative RT-PCR and adjusted to β-actin copies. $^{*}p = 0.02$ versus LPS-stimulated plaques, $^{\dagger}p = 0.04$ versus IL-17A–stimulated plaque tissue, and $^{\ddagger}p < 0.01$versus unstimulated plaque pieces.

ferentiate toward macrophages, DCs, or foam cells (1). As monocytes and monocyte-derived cells play a major role during atherogenesis and plaque destabilization (35), we thoroughly studied macrophage differentiation, specific macrophages transcriptome induced by IL-17A, and foam cell formation (19, 20). A recent study showed that IL-17A induced a monocyte-derived macrophage differentiation (36). The current study clearly shows that IL-17A has no effect on macrophage differentiation or foam cell formation. These contradictory findings may be due to different study protocols and IL-17A concentrations.

But using unbiased statistics as well as methods informed by current knowledge on macrophage polarization, we found that IL-17A induces a specific macrophage transcriptome that is characterized by upregulation of a large number of proinflammatory genes coding for cytokines and various chemokines implicated in atherogenesis like *IL6* or *CCL2*, as well as genes involved in oxidative stress such as metallothioneines. Interestingly, although being predominantly proinflammatory, the IL-17A–induced macrophage transcriptome showed similarities with the proinflammatory M1 macrophages but, at the same time, display characteristics that are in clear contradiction with the classical M1 polarization. Thus, upregulation of the hemoglobin scavenger receptor CD163 is usually associated with M2 polarization (19). These findings were supported by an upregulation of chemokines predominantly expressed by the IL-17A–induced macrophage subtype compared with M1, M2, and M4 within cultured plaque tissue samples. Taken together, these findings clearly show that IL-17A induces proinflammatory processes in human macrophages through induction of a specific macrophage phenotype, which may be associated with the proatherosclerotic effects of IL-17A. Furthermore, these data add to several studies published over the past years showing that atherosclerotic plaque macrophages do not represent a uniform entity but are composed of various subsets with distinct phenotypic and functional characteristics. Although Bouhlel et al. have demonstrated the presence of both gene transcripts associated with M1 and M2 polarization in human atherosclerotic plaques (37), other groups including ourselves have shown that further macrophage phenotypes can be identified within the arterial wall in atherosclerotic patients (20, 38). It is very likely that IL-17A also affects macrophages within atherosclerotic plaques. Further experiments are needed to specifically study how these effects specifically promote plaque progression or destabilization.

Apart from LPS, autoantigen oxLDLs found in the plaque environment are also candidates for TLR4-dependent activation of lesional monocyte-derived macrophages and DCs (39, 40). TLR4

Table V. Quantitative supernatant ELISA results for different cytokines and chemokines from plaque culture experiments

Variable (pg/ml)	Unstimulated (n = 10)	IL-17A (n = 10)	LPS (n = 10)	p Value Unstimulated versus IL-17A
IL-2	0	0	0	NS
IL-4	0	0	0	NS
IL-5	0	0	0	NS
IL-6	3.3	35.1	33	<0.0001
IL-10	0	0.3	0	NS
IL-12	0.3	0.4	0.5	NS
IL-13	0	0.1	3	NS
IFN-γ	0	0	4.7	NS
TGF-β	17	46.8	143	0.02
TNF-α	2.7	20.47	113	<0.0001
MCP-1 (CCL2)	1363	6886	5598	0.004
G-CSF	0	6.4	3.8	0.01

Data are shown as mean ± SD in picograms per milliliter.

is known to play a major role in plaque inflammatory activation. Methe et al. (41) showed that circulating monocytes during acute coronary syndrome overexpress TLR4, and TLR4-lacking Apoe$^{-/-}$ mice showed reduced atherosclerotic lesions (42). The current study shows that IL-17A sensitizes APC, cocultured with T cells, toward pathogen-derived TLR4 ligand oxLDL by upregulating various molecules of the Th1- and IL-17–expressing Th cell lineage, but not markers of the Th2 lineage. These effects do not derive from an IL-17A–dependent increased oxLDL uptake of macrophages. The in vitro findings were supported by an additive effect of IL-17A to LPS on cultured plaque tissue samples. Thus, IL-17A is also involved in Ag uptake–dependent immune response, a major step in atherogenesis and plaque instability.

In summary, IL-17A appears to be centrally involved in advanced atherosclerosis, most likely via proinflammatory changes at multiple levels such as chemoattraction, cell rolling and adhesion, cell activation/polarization, and sensitization of Ag presentation in the inflammatory cascade of atherosclerosis. Together with previous studies of our group and others, the current study underlines IL-17A as an independent important proatherogenic cytokine and warrants further experimental and clinical studies of this cytokine. Consequently, blocking IL-17A could be an attractive therapeutic approach for the prevention of atherosclerotic lesion progression.

Acknowledgments

We thank Nadine Wambsganss and Jutta Scheuerer for expert technical assistance.

Disclosures

The authors have no financial conflicts of interest.

References

1. Galkina, E., and K. Ley. 2009. Immune and inflammatory mechanisms of atherosclerosis (*). *Annu. Rev. Immunol.* 27: 165–197.
2. Robbins, C. S., I. Hilgendorf, G. F. Weber, I. Theurl, Y. Iwamoto, J. L. Figueiredo, R. Gorbatov, G. K. Sukhova, L. M. Gerhardt, D. Smyth, et al. 2013. Local proliferation dominates lesional macrophage accumulation in atherosclerosis. *Nat. Med.* 19: 1166–1172.
3. Gautier, E. L., C. Jakubzick, and G. J. Randolph. 2009. Regulation of the migration and survival of monocyte subsets by chemokine receptors and its relevance to atherosclerosis. *Arterioscler. Thromb. Vasc. Biol.* 29: 1412–1418.
4. Potteaux, S., E. L. Gautier, S. B. Hutchison, N. van Rooijen, D. J. Rader, M. J. Thomas, M. G. Sorci-Thomas, and G. J. Randolph. 2011. Suppressed monocyte recruitment drives macrophage removal from atherosclerotic plaques of Apoe$^{-/-}$ mice during disease regression. *J. Clin. Invest.* 121: 2025–2036.
5. Weaver, C. T., R. D. Hatton, P. R. Mangan, and L. E. Harrington. 2007. IL-17 family cytokines and the expanding diversity of effector T cell lineages. *Annu. Rev. Immunol.* 25: 821–852.
6. Yang, Y., J. Weiner, Y. Liu, A. J. Smith, D. J. Huss, R. Winger, H. Peng, P. D. Cravens, M. K. Racke, and A. E. Lovett-Racke. 2009. T-bet is essential for encephalitogenicity of both Th1 and Th17 cells. *J. Exp. Med.* 206: 1549–1564.
7. Erbel, C., L. Chen, F. Bea, S. Wangler, S. Celik, F. Lasitschka, Y. Wang, D. Böckler, H. A. Katus, and T. J. Dengler. 2009. Inhibition of IL-17A attenuates atherosclerotic lesion development in apoE-deficient mice. *J. Immunol.* 183: 8167–8175.
8. Smith, E., K. M. Prasad, M. Butcher, A. Dobrian, J. K. Kolls, K. Ley, and E. Galkina. 2010. Blockade of interleukin-17A results in reduced atherosclerosis in apolipoprotein E-deficient mice. *Circulation* 121: 1746–1755.
9. Chen, S., K. Shimada, W. Zhang, G. Huang, T. R. Crother, and M. Arditi. 2010. IL-17A is proatherogenic in high-fat diet-induced and *Chlamydia pneumoniae* infection-accelerated atherosclerosis in mice. *J. Immunol.* 185: 5619–5627.
10. Taleb, S., M. Romain, B. Ramkhelawon, C. Uyttenhove, G. Pasterkamp, O. Herbin, B. Esposito, N. Perez, H. Yasukawa, J. Van Snick, et al. 2009. Loss of SOCS3 expression in T cells reveals a regulatory role for interleukin-17 in atherosclerosis. *J. Exp. Med.* 206: 2067–2077.
11. Gistera, A., A. K. Robertson, J. Andersson, D. F. Ketelhuth, O. Ovchinnikova, S. K. Nilsson, A. M. Lundberg, M. O. Li, R. A. Flavell, and G. K. Hansson. 2013. Transforming Growth Factor-beta Signaling in T Cells Promotes Stabilization of Atherosclerotic Plaques Through an Interleukin-17-Dependent Pathway. *Sci. Transl. Med.* 5: 196ra100.
12. de Boer, O. J., J. J. van der Meer, P. Teeling, C. M. van der Loos, M. M. Idu, F. van Maldegem, J. Aten, and A. C. van der Wal. 2010. Differential expression of interleukin-17 family cytokines in intact and complicated human atherosclerotic plaques. *J. Pathol.* 220: 499–508.
13. Erbel, C., T. J. Dengler, S. Wangler, F. Lasitschka, F. Bea, N. Wambsganss, M. Hakimi, D. Böckler, H. A. Katus, and C. A. Gleissner. 2011. Expression of IL-17A in human atherosclerotic lesions is associated with increased inflammation and plaque vulnerability. *Basic Res. Cardiol.* 106: 125–134.
14. Celik, S., H. Langer, K. Stellos, A. E. May, V. Shankar, K. Kurz, H. A. Katus, M. P. Gawaz, and T. J. Dengler. 2007. Platelet-associated LIGHT (TNFSF14) mediates adhesion of platelets to human vascular endothelium. *Thromb. Haemost.* 98: 798–805.
15. Jain, N., J. Thatte, T. Braciale, K. Ley, M. O'Connell, and J. K. Lee. 2003. Local-pooled-error test for identifying differentially expressed genes with a small number of replicated microarrays. *Bioinformatics* 19: 1945–1951.
16. Gleissner, C. A., I. Shaked, C. Erbel, D. Böckler, H. A. Katus, and K. Ley. 2010. CXCL4 downregulates the atheroprotective hemoglobin receptor CD163 in human macrophages. *Circ. Res.* 106: 203–211.
17. Jain, N., H. Cho, M. O'Connell, and J. K. Lee. 2005. Rank-invariant resampling based estimation of false discovery rate for analysis of small sample microarray data. *BMC Bioinformatics* 6: 187.
18. Subramanian, A., P. Tamayo, V. K. Mootha, S. Mukherjee, B. L. Ebert, M. A. Gillette, A. Paulovich, S. L. Pomeroy, T. R. Golub, E. S. Lander, and J. P. Mesirov. 2005. Gene set enrichment analysis: a knowledge-based approach for interpreting genome-wide expression profiles. *Proc. Natl. Acad. Sci. USA* 102: 15545–15550.
19. Martinez, F. O., S. Gordon, M. Locati, and A. Mantovani. 2006. Transcriptional profiling of the human monocyte-to-macrophage differentiation and polarization: new molecules and patterns of gene expression. *J. Immunol.* 177: 7303–7311.
20. Gleissner, C. A., I. Shaked, K. M. Little, and K. Ley. 2010. CXC chemokine ligand 4 induces a unique transcriptome in monocyte-derived macrophages. *J. Immunol.* 184: 4810–4818.
21. Gordon, S. 2007. The macrophage: past, present and future. *Eur. J. Immunol.* 37 (Suppl 1): S9–S17.
22. Pöllinger, B., T. Junt, B. Metzler, U. A. Walker, A. Tyndall, C. Allard, S. Bay, R. Keller, F. Raulf, F. Di Padova, et al. 2011. Th17 cells, not IL-17+ γδ T cells, drive arthritic bone destruction in mice and humans. *J. Immunol.* 186: 2602–2612.
23. Niessner, A., M. S. Shin, O. Pryshchep, J. J. Goronzy, E. L. Chaikof, and C. M. Weyand. 2007. Synergistic proinflammatory effects of the antiviral cytokine interferon-alpha and Toll-like receptor 4 ligands in the atherosclerotic plaque. *Circulation* 116: 2043–2052.
24. Danzaki, K., Y. Matsui, M. Ikesue, D. Ohta, K. Ito, M. Kanayama, D. Kurotaki, J. Morimoto, Y. Iwakura, H. Yagita, et al. 2012. Interleukin-17A deficiency accelerates unstable atherosclerotic plaque formation in apolipoprotein E-deficient mice. *Arterioscler. Thromb. Vasc. Biol.* 32: 273–280.
25. Butcher, M. J., B. N. Gjurich, T. Phillips, and E. V. Galkina. 2012. The IL-17A/IL-17RA axis plays a proatherogenic role via the regulation of aortic myeloid cell recruitment. *Circ. Res.* 110: 675–687.
26. Madhur, M. S., S. A. Funt, L. Li, A. Vinh, W. Chen, H. E. Lob, Y. Iwakura, Y. Blinder, A. Rahman, A. A. Quyyumi, and D. G. Harrison. 2011. Role of interleukin 17 in inflammation, atherosclerosis, and vascular function in apolipoprotein e-deficient mice. *Arterioscler. Thromb. Vasc. Biol.* 31: 1565–1572.
27. Okamoto, Y., M. Hasegawa, T. Matsushita, Y. Hamaguchi, D. L. Huu, Y. Iwakura, M. Fujimoto, and K. Takehara. 2012. Potential roles of interleukin-17A in the development of skin fibrosis in mice. *Arthritis Rheum.* 64: 3726–3735.
28. Gregersen, I., M. Skjelland, S. Holm, K. B. Holven, K. Krogh-Sørensen, D. Russell, E. T. Askevold, C. P. Dahl, S. Ørn, L. Gullestad, et al. 2013. Increased systemic and local interleukin 9 levels in patients with carotid and coronary atherosclerosis. *PLoS ONE* 8: e72769.
29. Eid, R. E., D. A. Rao, J. Zhou, S. F. Lo, H. Ranjbaran, A. Gallo, S. I. Sokol, S. Pfau, J. S. Pober, and G. Tellides. 2009. Interleukin-17 and interferon-gamma are produced concomitantly by human coronary artery-infiltrating T cells and act synergistically on vascular smooth muscle cells. *Circulation* 119: 1424–1432.
30. Cheng, X., X. Yu, Y. J. Ding, Q. Q. Fu, J. J. Xie, T. T. Tang, R. Yao, Y. Chen, and Y. H. Liao. 2008. The Th17/Treg imbalance in patients with acute coronary syndrome. [Published erratum appears in 2009 *Clin. Immunol.* 133: 447.] *Clin. Immunol.* 127: 89–97.
31. Simon, T., S. Taleb, N. Danchin, L. Laurans, B. Rousseau, S. Cattan, J. M. Montely, O. Dubourg, A. Tedgui, S. Kotti, and Z. Mallat. 2013. Circulating levels of interleukin-17 and cardiovascular outcomes in patients with acute myocardial infarction. *Eur. Heart J.* 34: 570–577.
32. Shimada, M., A. Andoh, K. Hata, K. Tasaki, Y. Araki, Y. Fujiyama, and T. Bamba. 2002. IL-6 secretion by human pancreatic periacinar myofibroblasts in response to inflammatory mediators. *J. Immunol.* 168: 861–868.
33. Llodrá, J., V. Angeli, J. Liu, E. Trogan, E. A. Fisher, and G. J. Randolph. 2004. Emigration of monocyte-derived cells from atherosclerotic lesions characterizes regressive, but not progressive, plaques. *Proc. Natl. Acad. Sci. USA* 101: 11779–11784.
34. Williams, K. J., J. E. Feig, and E. A. Fisher. 2008. Rapid regression of atherosclerosis: insights from the clinical and experimental literature. *Nat. Clin. Pract. Cardiovasc. Med.* 5: 91–102.
35. Moore, K. J., and I. Tabas. 2011. Macrophages in the pathogenesis of atherosclerosis. *Cell* 145: 341–355.
36. Zizzo, G., and P. L. Cohen. 2013. IL-17 stimulates differentiation of human anti-inflammatory macrophages and phagocytosis of apoptotic neutrophils in response to IL-10 and glucocorticoids. *J. Immunol.* 190: 5237–5246.
37. Bouhlel, M. A., B. Derudas, E. Rigamonti, R. Dièvart, J. Brozek, S. Haulon, C. Zawadzki, B. Jude, G. Torpier, N. Marx, et al. 2007. PPARγ activation primes human monocytes into alternative M2 macrophages with anti-inflammatory properties. *Cell Metab.* 6: 137–143.

38. Waldo, S. W., Y. Li, C. Buono, B. Zhao, E. M. Billings, J. Chang, and H. S. Kruth. 2008. Heterogeneity of human macrophages in culture and in atherosclerotic plaques. *Am. J. Pathol.* 172: 1112–1126.
39. Xu, X. H., P. K. Shah, E. Faure, O. Equils, L. Thomas, M. C. Fishbein, D. Luthringer, X. P. Xu, T. B. Rajavashisth, J. Yano, et al. 2001. Toll-like receptor-4 is expressed by macrophages in murine and human lipid-rich atherosclerotic plaques and upregulated by oxidized LDL. *Circulation* 104: 3103–3108.
40. Kadowaki, N., S. Ho, S. Antonenko, R. W. Malefyt, R. A. Kastelein, F. Bazan, and Y. J. Liu. 2001. Subsets of human dendritic cell precursors express different toll-like receptors and respond to different microbial antigens. *J. Exp. Med.* 194: 863–869.
41. Methe, H., J. O. Kim, S. Kofler, M. Weis, M. Nabauer, and J. Koglin. 2005. Expansion of circulating Toll-like receptor 4-positive monocytes in patients with acute coronary syndrome. *Circulation* 111: 2654–2661.
42. Michelsen, K. S., M. H. Wong, P. K. Shah, W. Zhang, J. Yano, T. M. Doherty, S. Akira, T. B. Rajavashisth, and M. Arditi. 2004. Lack of Toll-like receptor 4 or myeloid differentiation factor 88 reduces atherosclerosis and alters plaque phenotype in mice deficient in apolipoprotein E. *Proc. Natl. Acad. Sci. USA* 101: 10679–10684.